research papers

The invariom model and its application: refinement of D,L-serine at different temperatures and resolution

B. Dittrich,* C. B. Hübschle, M. Messerschmidt, R. Kalinowski, D. Girnt and P. Luger

Institut für Chemie/Kristallographie der Freien Universität Berlin, Berlin, D-14195 Germany.
Correspondence e-mail: birger@chemie.fu-berlin.de

Three X-ray data sets of the same D,L-serine crystal were measured at temperatures of 298, 100 and 20 K. These data were then evaluated using invarioms and the Hansen & Coppens aspherical-atom model. Multipole populations for invarioms, which are pseudoatoms that remain approximately invariant in an intermolecular transfer, were theoretically predicted using different density functional theorem (DFT) basis sets. The invariom parameters were kept fixed and positional and thermal parameters were refined to compare the fitting against the multi-temperature data at different resolutions. The deconvolution of thermal motion and electron density with respect to data resolution was studied by application of the Hirshfeld test. Above a resolution of $\sin \theta / \lambda \approx 0.55$ Å^{-1}, or $d \approx 0.9$ Å, this test was fulfilled. When the Hirshfeld test is fulfilled, a successful modeling of the aspherical electron density with invarioms is achieved, which was proven by Fourier methods. Molecular geometry improves, especially for H atoms, when using the invariom method compared to the independent-atom model, as a comparison with neutron data shows. Based on this example, the general applicability of the invariom concept to organic molecules is proven and the aspherical density modeling of a larger biomacromolecule is within reach.

1. Introduction

Recently the concept of invarioms (Dittrich *et al.*, 2004) was introduced. By defining transferable pseudoatoms and using a database approach for theoretically predicted multipole populations, one can replace the independent-atom model (IAM) with an aspherical scattering model. For this purpose, the Hansen & Coppens (1978) aspherical-atom multipole formalism was chosen.

This invariom concept can be applied to all elements in the Periodic Table. It is based on the nearest-neighbor approximation (NNA), which was also used for crystallographic work in a recent paper by Koritsanszky *et al.* (2002). When applying the NNA, only a limited number of invarioms exists for each element. For modeling X-ray data, invarioms are assigned to each atom of an element type in a given crystal structure. Invariom-multipole populations are not refined and the total molecular density is obtained by summation of their contributions.

The application of this method leads to improved molecular geometry (atomic positions), especially for H atoms. It also leads to better figures of merit like a lower *R* factor and, owing to an improved scattering model, to more accurate phases than the use of the IAM. As the description of electron density allows for asphericity in contrast to the IAM, this approach results in improved deconvolution of thermal motion and electron density.

In this work, we studied the effect of different basis sets – projected by the multipole model – on the figures of merit of least-square refinements. Secondly, the physical meaning of the anisotropic displacement parameters (ADPs) was compared for the IAM and invariom models. Finally, the effect of data resolution on the figures of merit was investigated.

Three data sets were measured for the same crystal of D,L-serine at different temperatures using a newly developed measurement set-up (Messerschmidt *et al.*, 2003). This amino acid was the subject of an earlier charge-density study at 100 K (Flaig *et al.*, 1999). How far the multitemperature data can provide deeper insight into thermal motion description will be investigated in a following work.

2. Density modeling using invarioms

2.1. Invariom modeling in perspective with other current work

The first work that appeared on the transfer of pseudoatom parameters extracted physically meaningful anisotropic displacement parameters (ADPs) for naphthalene and

anthracene using high-resolution data for perylene (Brock *et al.*, 1991).

Apart from the definition and the introduction of notation for intramolecular transferable atoms, and the use of theoretical multipole parameters, our procedure is similar to the one described for experimental data by Pichon-Pesme *et al.* (1995). This group pioneered the transfer of amino acid and oligopeptide multipolar parameters to protein data (Jelsch *et al.*, 1998, 2000) and wrote software to refine the charge density of proteins at subatomic resolution (Guillot *et al.*, 2001).

The invariom procedure is similar to the one used in recent work by Volkov, Li, Koritsánszky & Coppens (2004), who also build a pseudoatom database from theoretical data. The performance of the database approach to reproduce the electron density and electrostatic properties of three amino acids in comparison to theoretical calculations is evaluated. Recent work shows that a new database based method (EP/MM) is superior to force-field approaches in the calculation of intermolecular electrostatic interaction energies (Volkov, Koritsánszky & Coppens, 2004). However, in the work of Volkov, Li, Koritsánszky & Coppens, populations are averaged over different model compounds so the deviation from electroneutrality might be different to results using our invariom database, where only one model compound is used for each invariom.

2.2. The multipole model

Experimental data sets were modeled using the Hansen & Coppens (1978) multipole formalism as implemented in the program package *XD* (Koritsánszky *et al.*, 2003). The formalism allows a pseudoatom representation of deformations of the electron density $\rho(\mathbf{r})$ due to chemical bonding, and is described in detail by Coppens (1997). The total electron density is the sum of a spherical core, a spherical valence and an aspherical valence density:

$$\rho_{atom}(\mathbf{r}) = \rho_{core}(r) + P_{valence}\kappa^3\rho_{valence}(\kappa r)$$
$$+ \sum_{l=0}^{l_{max}} \kappa'^3 R_l(\kappa'\mathbf{r}) \sum_{m=0}^{l} P_{lm\pm}d_{lm\pm}(\theta, \phi). \quad (1)$$

l is the order of the multipole expansion. P's, κ and κ' are refinable multipole parameters, R are radial functions and d_{lm} are the orientation-dependent spherical harmonic deformation functions. When invarioms are used, the multipole parameters are not refined against experimental data but are taken from a database of theoretical parameters and kept constant in the least-squares refinement of positional and thermal parameters.

2.3. The construction of the database

The procedure for the construction of a database of theoretically derived multipole populations, and their notation, is briefly described in our recent paper (Dittrich *et al.*, 2004) and detailed here. So far the database is limited to atoms common to organic chemistry (H, C, N, O, S, P). The first step in the construction of the database was the prediction of all possible invarioms. Then model compounds that mimicked the

direct chemical environment (atomic number of the neighbor and bond order) of the atoms to which the invarioms related were created by replacing next-nearest neighbors with H atoms. In the case of mesomeric or delocalized systems, a further shell of atoms was taken into account in the model compounds. A geometry optimization using the *Gaussian* program (Frisch *et al.*, 1998) followed. Later in this work, we compare the performance of different basis sets that were employed. At this stage, the geometry and the electron density of the model-compound molecules for a chosen basis set were available. Theoretical structure factors were calculated from the *Gaussian* wavefunctions for the model compounds by analytical Fourier transform of the *Gaussian* orbital products (Chandler & Spackman, 1978) to subdivide the molecular electron density into invarioms or pseudoatoms. These structure factors were generated with the program *Tonto* (Jayatilaka & Grimwood, 2003) for reciprocal-lattice points of a cubic cell of 15 Å up to a resolution of $\sin\theta/\lambda = 1.15$ Å^{-1} using the centrosymmetric space group $P\bar{1}$. The central atoms were placed at $\frac{1}{4}, \frac{1}{4}, \frac{1}{4}$. The contribution of the core electrons was included in structure-factor calculations. With these structure factors, and the geometry from the optimization, the least-squares procedure yielded invariomic multipole populations that were stored in the database together with orientation and symmetry of the invariom's local atomic coordinate system. A molecular electroneutrality constraint was applied in the least-squares refinements and the hexadecapolar level of the multipole expansion was used for all atoms.

2.4. Invariom notation

We previously proposed a notation for invarioms, which is detailed below (see Fig. 1) using the example of serine. The element symbol of the atom of interest commences the name in capital letters, then the formal bond order and the nearest neighbors follow in lowercase letters ordered by their position in the Periodic Table (heavier atoms first). The order of the ligands is determined by their decreasing bond order. In the case of mesomerism or in delocalized systems, a bond order of 1.5 is specified. For these cases, the next-nearest neighbor has to be taken into account for the name. This is achieved by writing the next-nearest neighbors according to the previous
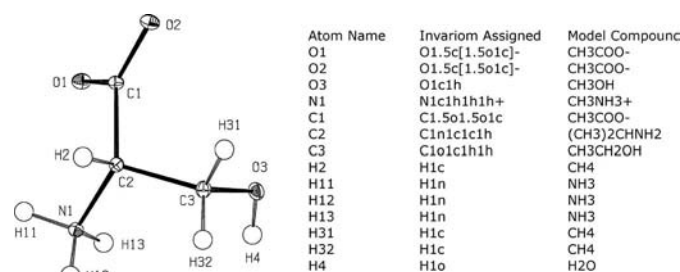

Figure 1
ORTEP representation (Burnett & Johnson, 1996) of the serine molecular structure in the crystal at 20 K with atomic numbering scheme, invariom names and corresponding model compounds. Thermal ellipsoids at 50% probability.

Table 1
Crystal and structure refinement data for D,L-serine at different temperatures.

Empirical formula	$C_3H_7NO_3$		
Formula weight (g mol^{-1})	105.09		
Cell setting, space group, Z	Monoclinic, $P2_1/a$ (No. 14), 4		
Temperature	298 K	100 K	20 K
Unit-cell dimensions:			
a (Å)	10.736 (1)	10.762 (1)	10.776 (1)
b (Å)	9.146 (1)	9.177 (1)	9.195 (1)
c (Å)	4.830 (1)	4.788 (1)	4.779 (1)
β (°)	106.46 (1)	106.76 (1)	106.87 (1)
V (Å^3)	454.8 (1)	452.8 (1)	453.1 (1)
Calculated density (g cm^{-3})	1.5348	1.5416	1.5405
$F(000)$	224.0		
Crystal size (mm)	$0.5 \times 0.45 \times 0.35$		
Crystal form, color	Rectangular, colorless		
Wavelength λ (Å)	0.7107		
Absorption coefficient μ (mm^{-1})	0.14		
Absorption correction	None		
Max. 2θ (°)	88.5	114.6	114.5
$(\sin\theta/\lambda)_{max}$ (Å^{-1})	0.985	1.184	1.183
No. of measured reflections	25178	38455	38628
No. of independent reflections	3551	5146	5136
No. of observed reflections	2703	4109	4292
Criterion for observed reflections	$I > 2\sigma(I)$		
Overall completeness	95.7%	79.4%	79.7%
Redundancy	6.9	7.0	6.9
Weighting scheme	Based on measured s.u.'s†		
$R_{int}(F^2)$‡	2.28%	2.89%	2.68%

† $w = 1/\sigma^2$.   ‡ $R_{int}(F^2) = \sum |F_o^2 - F_o^2(\text{mean})| / \sum F_o^2$.

rules in brackets after the nearest neighbors. For chiral invarioms, R or S is used as a prefix (CIP rules), separated by a dash. As only next-nearest neighbors are considered, chiral invarioms occur less frequently than chiral atoms. Finally, a $+$ or a $-$ indicates a charge. The sign is best placed at the very end of the name.[1]

2.5. The preprocessor invariomtool

It is emphasized that invarioms can now be automatically identified in a molecule from its geometry in a given crystal structure. We have written a preprocessor (Hübschle & Dittrich, 2004) that reads *XD* system files. It has a purpose similar to the program *LSDB* (Volkov, Li, Koritsánzky & Coppens, 2004). To locate bonds, the program looks for pairs of atoms, where the following equation (2) holds; d is the distance between the atoms, r_c is the covalent radius and EN the Allred–Rochow electronegativity (Allred & Rochow, 1958).

$$d \times 0.85 \leq r_c(\text{atom 1}) + r_c(\text{atom 2})$$
$$- 0.08|\text{EN}(\text{atom 1}) - \text{EN}(\text{atom 2})|. \quad (2)$$

To differentiate between single, mesomeric, double and triple bonds, the absolute value of this difference is evaluated. The program then assigns a unique invariom name to each atom in a crystal structure, taking into account its bonding situation.

From that invariom name, the corresponding multipole populations are located in the database and automatically transferred to each atom, using the same local atomic site symmetry as and a similar coordinate system to the database entry. When necessary, the program automatically creates dummy atoms for the atom of interest. Electroneutrality is achieved by adding the averaged charge difference between the neutral molecule and the sum of the invariom monopole populations to each atom. The preprocessor allows a wide
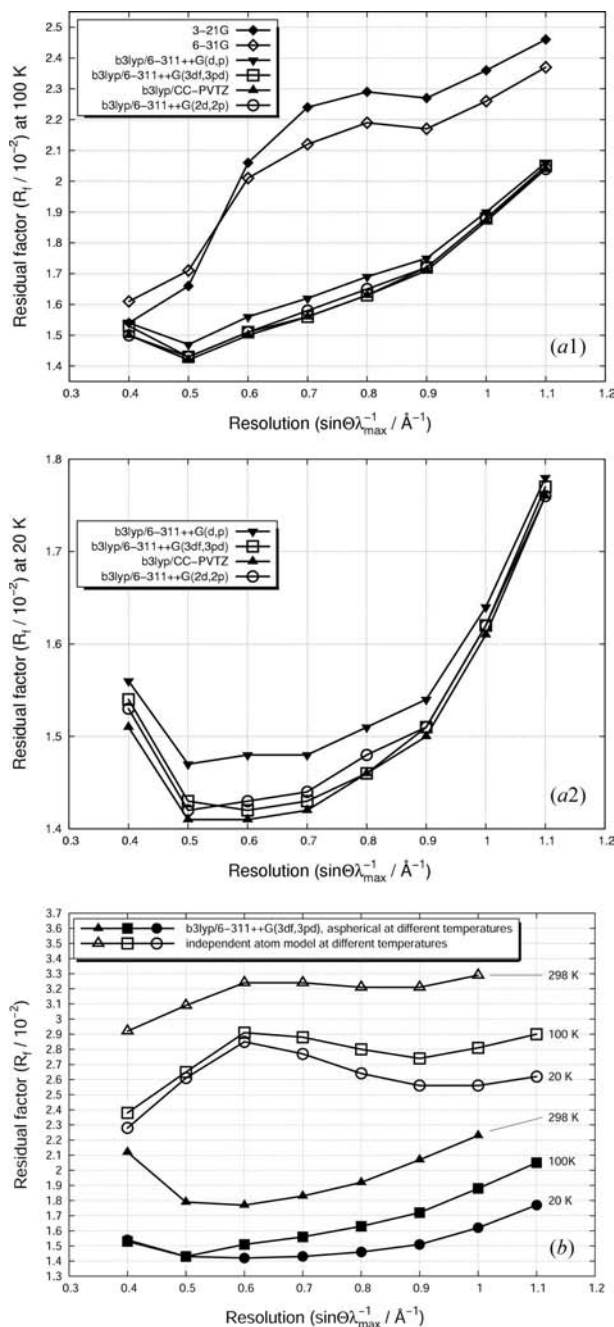
Figure 2
R factor plotted *versus* resolution for different basis sets using ($a1$) the 100 K and ($a2$) the 20 K data. (b) Comparison of the IAM and the invariom approximation for all temperatures for the basis set B3LYP/6–311++G(3df, 3pd).

[1] For the model compound of a carbon invariom assigned to any atom of a benzene ring, it is advantageous to calculate the complete ring instead of a radical. We are currently investigating mesomeric or delocalized systems and results will be reported in a following paper.

Table 2
Neutron bond lengths of D,L-serine compared to X-ray invariom and IAM model results at room temperature.

Bond	Distance (N)	Distance (X, invariom)		Distance (X, IAM)	
		$\sin\theta/\lambda = 0.98$ Å^{-1}	$\sin\theta/\lambda = 0.6$ Å^{-1}	$\sin\theta/\lambda = 0.98$ Å^{-1}	$\sin\theta/\lambda = 0.6$ Å^{-1}
O(1)—C(1)	1.248 (1)	1.2487 (5)	1.248 (2)	1.2479 (7)	1.246 (2)
O(2)—C(1)	1.257 (1)	1.2585 (5)	1.257 (2)	1.2586 (8)	1.256 (2)
O(3)—C(3)	1.414 (1)	1.4150 (5)	1.414 (2)	1.4172 (8)	1.417 (2)
O(3)—H(4)	0.981 (1)	0.95 (1)	0.97 (2)	0.92 (2)	0.92 (3)
N(1)—C(2)	1.487 (1)	1.4884 (5)	1.488 (2)	1.4883 (7)	1.490 (2)
N(1)—H(11)	1.037 (1)	1.048 (9)	1.05 (2)	0.96 (2)	0.94 (2)
N(1)—H(12)	1.045 (1)	1.03 (1)	1.03 (2)	0.95 (2)	0.96 (2)
N(1)—H(13)	1.041 (1)	1.03 (1)	1.02 (2)	0.94 (2)	0.94 (2)
C(1)—C(2)	1.531 (1)	1.5316 (5)	1.532 (2)	1.5291 (7)	1.528 (2)
C(2)—C(3)	1.518 (1)	1.5201 (5)	1.519 (2)	1.5165 (8)	1.514 (2)
C(2)—H(2)	1.101 (1)	1.080 (7)	1.07 (2)	0.956 (9)	0.93 (2)
C(3)—H(31)	1.095 (1)	1.096 (9)	1.10 (2)	0.97 (2)	0.97 (2)
C(3)—H(32)	1.095 (1)	1.121 (9)	1.12 (2)	1.00 (2)	0.98 (2)

application of the invariom concept to any organic molecule containing the elements given above and testing on other structures is in progress.

2.6. Density modeling

For the density modeling, each atom in the crystal structure was assigned an invariom. The total density of the molecule was then obtained by a superposition of invariom densities. In an invariom least-squares refinement, the database multipole parameters assigned to the atoms were, as mentioned before, not refined. The number of refined parameters therefore does not increase and application to low-resolution structures becomes feasible. Only a scale factor, positional and thermal parameters were refined.

3. Experimental

The molecular structure, thermal movement at 20 K and the atomic numbering scheme are shown in Fig. 1.

Three single-crystal diffraction experiments were carried out using the same crystal of the title compound on a Huber diffractometer (400 mm Eulerian cradle with offset χ circle) equipped with a double-stage helium cryostat and a Bruker APEX CCD detector. Data sets were collected at temperatures of 298, 100 and 20 K.[2] In the case of the 298 K data, the reciprocal space was explored by a combination of different ϕ scans with 2θ at −20 and −28° (radiation time 5 s) for measuring low-order reflections and −58° (30 s) for a medium-resolution shell. For the two low-temperature data sets, additional scans with −80° (120 s) were added.

In each of these runs, 1100 frames were collected and the sample-to-detector distance was 5.5 cm, except for a last high-order run for the low-temperature data where it was 4.5 cm. The scan width was 0.3° in all cases. An overall coverage of more than 95% up to a resolution of approximately 1 Å^{-1} in $\sin\theta/\lambda$ was obtained for the three data sets. No significant

intensity decay was observed. *Sortav* (Blessing, 1995) was used for scaling of runs, neglecting absorption. Further details of crystal data and measurement conditions are given in Table 1.

4. Results and discussion

We find that structural refinement using aspherical density parameters leads to an improved molecular geometry, and to the removal of systematic errors of X-ray diffraction studies. Asphericity shifts (Coppens *et al.*, 1969), which appear in, for example, longer C—O bonds due to spherical averaging over the oxygen valence density in the IAM at low resolution, are corrected for, although the differences are within the error range of the least-squares refinement. More importantly, errors in H-atom positions due to lack of hydrogen core density also disappear. The improvement of molecular geometry for D,L-serine using invariom is shown by comparison of bond distances of the 298 K X-ray invariom data to room-temperature neutron study results (Frey *et al.*, 1973) for different resolutions in Table 2.

The use of generalized X-ray scattering factors of pseudo-atoms (Stewart *et al.*, 1975) to obtain improved time averaged proton positions was first proposed by Stewart. For all temperatures, the use of invariom for aspherical-atom modeling leads to better figures of merit. A lower R factor, significantly reduced residual electron density and a better deconvolution of electron density and thermal motion can be achieved.

Figs. 2(*a*1) and (*a*2) show the crystallographic R factor plotted against different resolution shells for the different basis sets. The most significant improvement is seen for the standard basis sets B3LYP/6–311++G(2d, 2p), B3LYP/6–311++G(3df, 3pd) and the correlation consistent B3LYP/CC-PVTZ, which perform almost equally well. This holds for the 100 K data (*a*1) as well as the 20 K (*a*2) data, where the basis sets 3–21G and 6–31G are omitted for clarity. As the projection of the density by the multipole model is limited due to the radial functions employed, we decided to focus on the basis set B3LYP/6–311++G(3df, 3pd) from now on.

---

[2] Supplementary data for this paper are available from the IUCr electronic archives (Reference: CN5001). Services for accessing these data are described at the back of the journal.

Table 3
Figures of merit for invariom fit using basis set B3LYP/6-311++G(3df, 3pd) at different resolution shells and comparison to IAM (*italic*).

$\sin\theta/\lambda$ (Å^{-1})																
0.4		0.5		0.6		0.7		0.8		0.9		1.0†		1.1	
298 K															
$R(F)$ (%)	2.1	*2.9*	1.8	*3.1*	1.8	*3.2*	1.8	*3.2*	1.9	*3.2*	2.1	*3.2*	2.2	*3.3*		
$R_{all}(F)$ (%)	15.7	*28.1*	4.6	*7.5*	3.7	*6.1*	3.6	*4.9*	3.6	*4.7*	3.5	*4.6*	3.5	*4.5*		
$R_w(F)$ (%)	3.0	*3.7*	2.6	*4.1*	2.5	*4.1*	2.4	*4.0*	2.4	*3.9*	2.5	*3.9*	2.6	*3.9*		
DMSDA‡	46.833	*106.500*	12.167	*18.333*	6.167	*12.833*	4.167	*9.167*	3.333	*7.333*	2.667	*6.333*	2.667	*5.833*		
GoF	3.923	*4.773*	2.727	*4.189*	2.163	*3.600*	1.837	*3.053*	1.627	*2.616*	1.475	*2.293*	1.389	*2.110*		
Min. r. d.§	−0.133	*−0.170*	−0.172	*−0.234*	−0.189	*−0.260*	−0.189	*−0.269*	−0.187	*−0.282*	−0.196	*−0.299*	−0.205	*−0.309*		
Max. r. d.	0.147	*0.175*	0.164	*0.201*	0.173	*0.202*	0.171	*0.246*	0.176	*0.283*	0.190	*0.290*	0.195	*0.295*		
RMS r. d.	0.053	*0.060*	0.060	*0.076*	0.062	*0.078*	0.062	*0.078*	0.062	*0.078*	0.062	*0.079*	0.063	*0.079*		
100 K															
$R(F)$ (%)	1.5	*2.4*	1.4	*2.6*	1.5	*2.9*	1.6	*2.9*	1.6	*2.8*	1.7	*2.7*	1.9	*2.8*	2.1	*2.9*
$R_{all}(F)$ (%)	10.0	*19.6*	7.5	*13.4*	5.3	*8.4*	4.3	*5.6*	4.0	*5.0*	3.6	*4.6*	3.5	*4.4*	3.5	*4.3*
$R_w(F)$ (%)	1.7	*2.5*	1.7	*3.0*	1.7	*3.3*	1.8	*3.2*	1.8	*3.1*	1.9	*3.1*	2.0	*3.1*	2.1	*3.1*
DMSDA	47.500	*89.167*	14.667	*20.000*	6.500	*12.333*	3.667	*9.167*	2.667	*7.500*	2.000	*5.667*	1.167	*4.667*	1.500	*4.000*
GoF	2.106	*3.118*	1.589	*2.834*	1.411	*2.743*	1.331	*2.437*	1.262	*2.147*	1.177	*1.914*	1.193	*1.823*	1.176	*1.721*
Min. r. d.	−0.104	*−0.143*	−0.119	*−0.191*	−0.129	*−0.232*	−0.144	*−0.242*	−0.157	*−0.318*	−0.166	*−0.374*	−0.184	*−0.403*	−0.205	*−0.456*
Max. r. d.	0.133	*0.155*	0.141	*0.171*	0.150	*0.187*	0.159	*0.306*	0.162	*0.326*	0.182	*0.324*	0.205	*0.364*	0.210	*0.397*
RMS r. d.	0.044	*0.053*	0.047	*0.064*	0.047	*0.065*	0.048	*0.066*	0.049	*0.068*	0.051	*0.070*	0.053	*0.072*	0.055	*0.074*
20 K															
$R(F)$ (%)	1.5	*2.3*	1.4	*2.6*	1.4	*2.9*	1.4	*2.8*	1.5	*2.6*	1.5	*2.6*	1.6	*2.6*	1.8	*2.6*
$R_{all}(F)$ (%)	20.0	*45.2*	5.3	*10.6*	4.3	*7.4*	3.5	*5.0*	3.1	*4.3*	2.9	*3.8*	2.8	*3.6*	2.7	*3.6*
$R_w(F)$ (%)	1.9	*2.8*	2.0	*3.4*	1.8	*3.5*	1.8	*3.3*	1.7	*3.1*	1.8	*3.0*	1.9	*3.0*	2.0	*3.0*
DMSDA	71.333	*109.500*	14.833	*22.167*	5.833	*10.000*	3.333	*8.167*	2.500	*7.167*	1.500	*5.333*	1.333	*3.833*	1.333	*3.500*
GoF	2.464	*3.588*	1.928	*3.332*	1.646	*3.115*	1.463	*2.731*	1.346	*2.390*	1.251	*2.131*	1.252	*2.001*	1.237	*1.891*
Min. r. d.	−0.099	*−0.147*	−0.120	*−0.213*	−0.140	*−0.244*	−0.141	*−0.279*	−0.145	*−0.324*	−0.158	*−0.379*	−0.184	*−0.428*	−0.197	*−0.488*
Max. r. d.	0.124	*0.143*	0.136	*0.166*	0.155	*0.227*	0.165	*0.352*	0.166	*0.381*	0.178	*0.382*	0.200	*0.388*	0.213	*0.441*
RMS r. d.	0.039	*0.048*	0.044	*0.061*	0.046	*0.065*	0.047	*0.067*	0.048	*0.069*	0.050	*0.072*	0.051	*0.073*	0.054	*0.076*

† Full resolution of 0.98 Å^{-1} for room-temperature data. ‡ DMSDA: $[(\sum_i |DMSDA_i|)n^{-1}]/10^{-4}$, n is the number of bonds, DMSDA is the difference of mean-square displacement amplitudes. § r. d.: residual density

In Fig. 2(b), the test is repeated for all three temperatures and includes the IAM for comparison. The R factor is approximately constant for different resolution shells. For high resolution, it increases slightly, most visibly for the room-temperature refinements, probably due to noise in the data. For the 20 K data, this also holds, indicating another effect of small differences between the experimentally measured and the structure factors calculated from the invariom database, which will be discussed for Fig. 3.

Other figures of merit of different resolution shells, and values that show the dependence of the residual electron density on data resolution, are given in Table 3. At low resolution, the improvement is not significant, while for higher resolution, starting from 0.6 Å^{-1} in $\sin\theta/\lambda$, an improvement can be seen. While for the IAM (included in *italic* type for the different temperatures) the positive residual density at 20 K can be as high as 0.44 e Å^{-3}, it is reduced to 0.21 e Å^{-3} using invarioms even for full resolution. The reduction of residual electron density is similar for the other data sets and resolution cut-offs. These differences can be visualized by calculation of a residual density map with Fourier methods.

Fourier map Fig. 3(a) was calculated from the room-temperature data using all reflections above $2\sigma(F)$. Already an accumulation of electron density in covalent bonds is visible. For the 20 K data set, which is of very good quality, no features of residual electron density are visible at a medium resolution of $\sin\theta/\lambda = 0.7$ Å^{-1} (Fig. 3b) when invariom multipole parameters are used. When all reflections are included, small differences between the density calculated using the database entries and the Fourier transform of the high-resolution data become evident (Fig. 3c). We are currently trying to better understand the nature of these differences. These are probably due to the crystal-field effect, but could be due to the nearest- or next-

Figure 3
Residual density in the main molecular plane. (a) Room-temperature data without resolution cut-off and IAM. (b) Invariom transfer using 20 K data and cut-off at 0.7 Å^{-1}. (c) Invariom transfer, 20 K data and cut-off at 1.1 Å^{-1}. Contours at 0.05 e Å^{-3}.

nearest-neighbor approximation, or shortcomings in the theoretical calculations. It can be concluded that, for standard data sets of medium and even high resolution, the fit of the theoretical multipole parameters is excellent.

Fig. 4 shows the effect of the inclusion of the aspherical density on the anisotropic temperature parameters with respect to data resolution. To better describe the improvements, we use the Hirshfeld test (Hirshfeld, 1976), which indicates if thermal parameters are physically meaningful. The bond-projected mean-square displacement amplitudes of bonded atoms of similar mass should be comparable.

Temperature parameters for C, N and O atoms are not considered to include bonding effects if the difference of the mean square displacement amplitudes (DMSDA) is smaller than 0.001 Å^2. In our study, we use a mean DMSDA value for the six non-hydrogen bonds. This value is plotted against resolution for the basis set B3LYP/6–311++G(3df, 3pd) in Fig. 4 and is also included in Table 3. Starting from a resolution of 0.55 Å^{-1} in $\sin\theta/\lambda$ (or $d = 0.9 \text{ Å}$), the Hirshfeld test is fulfilled for all temperatures when invarioms are used. In the IAM, also included in Fig. 4, the deconvolution does not work properly and the test is not fulfilled at that resolution.

Effects of the crystal field on the electron-density distribution, mainly due to hydrogen bonding, are generally not included in the theoretically predicted multipole populations obtained from isolated molecules. Nevertheless, it is well known that these effects can significantly influence the density. This methodological shortcoming can be overcome when the data-to-parameter ratio is sufficient to refine the multipole populations of the non-H atoms involved in hydrogen bonding. In this study, we did not further investigate crystal-field effects.

5. Conclusions

By using invariomic aspherical scattering factors, the systematic positional errors of H atoms in X-ray diffraction studies can be avoided and all positional parameters improve.
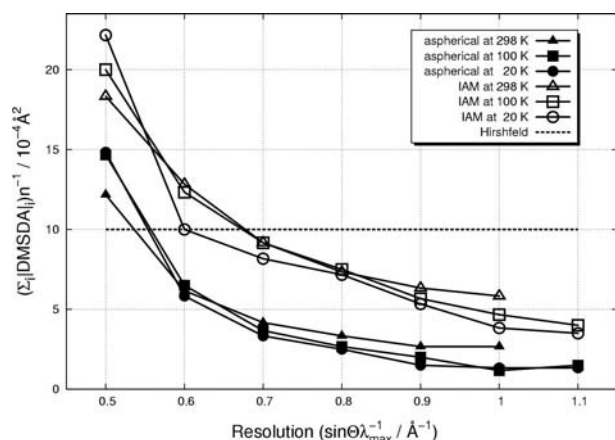

Figure 4
Mean value for bonds between C, N and O atoms for the Hirshfeld test plotted *versus* resolution. Above $10 \times 10^{-4} \text{ Å}^2$ (dotted line), the test is not considered fulfilled, as suggested by Hirshfeld.

The use of invarioms is therefore recommended for data sets of organic molecules of different resolution and at all temperatures. Low-temperature data are preferred, although the procedure can successfully be applied to room-temperature data. Modeling is straightforward using the preprocessor program and allows accurate and high-throughput invariom density studies. Such studies can be performed quickly without the need for well diffracting high-symmetry or centrosymmetric crystals, usually a prerequisite for charge-density studies. Still only the refinement of multipole parameters allows one to determine *e.g.* crystal field effects that are not included in the invariom density.

Compared to the IAM, invariom modeling employs a more accurate (aspherical) electron density and overcomes the IAM's shortcomings. The resolution requirement for data considered to be useful is similar to that from which anisotropic temperature factors can be refined. We recommend that resolutions higher than $\sin\theta/\lambda = 0.5 \text{ Å}^{-1}$ (or $d = 1.0 \text{ Å}$) are used, as anisotropic thermal parameters then become physically meaningful. An application to ultra high resolution protein or other supramolecular data is within reach.

References

Allred, A. L. & Rochow, E. G. (1958). *J. Inorg. Nucl. Chem.* **5**, 264–268.

Blessing, R. H. (1995). *Acta Cryst.* A**51**, 33–38.

Brock, C. P., Dunitz, J. D. & Hirshfeld, F. L. (1991). *Acta Cryst.* B**47**, 789–797.

Burnett, M. N. & Johnson, C. K. (1996). *ORTEPIII, Oak Ridge Thermal Ellipsoid Plot Program for Crystal Structure Illustrations*. Tech. Rep. ORNL-6895, Oak Ridge National Laboratory, Oak Ridge, Tennessee, USA.

Chandler, G. S. & Spackman, M. A. (1978). *Acta Cryst.* A**34**, 341–343.

Coppens, P. (1997). *X-ray Charge Densities and Chemical Bonding. IUCr Texts on Crystallography*, No. 4. Oxford University Press.

Coppens, P., Sabine, T. M., Delaplane, R. G. & Ibers, J. A. (1969). *Acta Cryst.* B**25**, 2451–2458.

Dittrich, B., Koritsánszky, T. & Luger, P. (2004). *Angew. Chem. Int. Ed. Engl.* **43**, 2718–2721.

Flaig, R., Koritsánszky, T., Janczak, J., Krane, H.-G., Morgenroth, W. & Luger, P. (1999). *Angew. Chem. Int. Ed. Engl.* **38**, 1397–1400.

Frey, M. N., Lehmann, M. S., Koetzle, T. F. & Hamilton, W. C. (1973). *Acta Cryst.* B**29**, 876–884.

Frisch, M. J., Trucks, G. W., Schlegel, H. B., Scuseria, G. E., Robb, M. A., Cheeseman, J. R., Zakrzewski, V. G. Jr, Stratmann, R. E., Burant, J. C., Dapprich, S., Millam, J. M., Daniels, A. D., Kudin, K. N., Strain, M. C., Farkas, O., Tomasi, J., Barone, V., Cossi, M., Cammi, R., Mennucci, B., Pomelli, C., Adamo, C., Clifford, S., Ochterski, J., Petersson, G. A., Ayala, P. Y., Cui, Q., Morokuma, K., Malick, D. K., Rabuck, A. D., Raghavachari, K., Foresman, J. B., Cioslowski, J., Ortiz, J. V., Baboul, A. G., Stefanov, B. B., Liu, G., Liashenko, A., Piskorz, P., Komaromi, I., Gomperts, R., Martin, R. L., Fox, D. J., Keith, T., Al-Laham, M. A., Peng, C. Y.,

Nanayakkara, A., Gonzalez, C., Challacombe, M., Gill, P. M. W., Johnson, B., Chen, W., Wong, M. W., Andres, J. L., Gonzalez, C., Head-Gordon, M., Replogle, E. S. & Pople, J. A. (1998). *Gaussian 98, Revision A.7.* Tech. Rep., Gaussian, Inc., Pittsburgh, PA, USA.

Guillot, B., Viry, L., Guillot, R., Lecomte, C. & Jelsch, C. (2001). *J. Appl. Cryst.* **34**, 214–223.

Hansen, N. K. & Coppens, P. (1978). *Acta Cryst.* A**34**, 909–921.

Hirshfeld, F. L. (1976). *Acta Cryst.* A**32**, 239–244.

Hübschle, C. B. & Dittrich, B. (2004). *Invariomtool, a Preprocessor Program for Aspherical Atom Modeling with XD using Invarioms.* Tech. Rep., Freie Universität Berlin, Berlin, Germany.

Jayatilaka, D. & Grimwood, D. J. (2003). *Comput. Sci. ICCS 2003*, **2660**, 142–151.

Jelsch, C., Pichon-Pesme, V., Lecomte, C. & Aubry, A. (1998). *Acta Cryst.* D**54**, 1306–1318.

Jelsch, C., Teeter, M. M., Lamzin, V., Pichon-Pesme, V., Blessing, R. H. & Lecomte, C. (2000). *Proc. Natl Acad. Sci. USA*, **97**, 3171–3176.

Koritsánszky, T., Richter, T., Macci, P., Gatti, C., Howard, S., Mallinson, P. R., Farrugia, L., Su, Z. W. & Hansen, N. K. (2003). *XD – a Computer Program Package for Multipole Refinement and Analysis of Electron Densities from Diffraction Data.* Tech. Rep., Freie Universität Berlin, Berlin, Germany.

Koritsanszky, T., Volkov, A. & Coppens, P. (2002). *Acta Cryst.* A**58**, 464–472.

Messerschmidt, M., Meyer, M. & Luger, P. (2003). *J. Appl. Cryst.* **36**, 1452–1454.

Pichon-Pesme, V., Lecomte, C. & Lachekar, H. (1995). *J. Phys. Chem.* **99**, 6242–6250.

Stewart, R. F., Bentley, J. & Goodman, B. (1975). *J. Phys. Chem.* **63**, 3786–3793.

Volkov, A., Koritsánzky, T. & Coppens, P. (2004). *Chem. Phys. Lett.* **391**, 170–175.

Volkov, A., Li, X., Koritsánzky, T. & Coppens, P. (2004). *J. Phys. Chem. A*, **108**, 4283–4300.